

$\eta, \eta' \rightarrow \pi^+ \pi^- l^+ l^-$ in a chiral unitary approach

B. Borasoy¹, R. Nißler²

Helmholtz-Institut für Strahlen- und Kernphysik (Theorie)
Universität Bonn
Nussallee 14-16, D-53115 Bonn, Germany

Abstract

The decays $\eta, \eta' \rightarrow \pi^+ \pi^- l^+ l^-$ (with $l = e, \mu$) are investigated within a chiral unitary approach which combines the chiral effective Lagrangian with a coupled-channels Bethe-Salpeter equation. Predictions for the decay widths and spectra are given.

PACS: 13.20.Jf, 12.39.Fe

Keywords: Chiral Lagrangians, chiral anomaly, unitarity.

¹email: borasoy@itkp.uni-bonn.de

²email: rnissler@itkp.uni-bonn.de

1 Introduction

The decays $\eta^{(\prime)} \rightarrow \pi^+ \pi^- l^+ l^-$ are interesting in several respects. First, they involve contributions from the box-anomaly of quantum chromodynamics. Second, they probe the transition form factors of the η and η' . In principle, the decays are suited to test whether double vector meson dominance is indeed realized in nature, which is also an important issue for the anomalous magnetic moment of the muon and kaon decays [1]. Moreover, since the η' is closely related to the axial U(1) anomaly of the strong interactions, one can study the phenomenological implications of the anomaly at low energies.

On the experimental side, there is renewed interest in η, η' decays which are investigated at WASA@COSY [2], MAMI [3], KLOE [4, 5] and by the VES collaboration [6, 7]. There is thus the necessity to provide a consistent and uniform theoretical description for these decays.

In this respect, the combination of the chiral effective Lagrangian which incorporates the symmetries and symmetry-breaking patterns of QCD in combination with a coupled-channels Bethe-Salpeter equation (BSE) that takes into account final-state interactions in the decays and satisfies exact two-body unitarity has been proven very useful. In a series of papers, this approach has been successfully applied to the hadronic decay modes of η and η' [8–10], and the anomalous decays $\eta^{(\prime)} \rightarrow \gamma^{(*)} \gamma^{(*)}$ [11] and $\eta^{(\prime)} \rightarrow \pi^+ \pi^- \gamma$ [12].

Of particular interest is the last work [12] which we extend here to off-shell photons since the process $\eta^{(\prime)} \rightarrow \pi^+ \pi^- l^+ l^-$ can be regarded as the two-step process $\eta^{(\prime)} \rightarrow \pi^+ \pi^- \gamma^* \rightarrow \pi^+ \pi^- l^+ l^-$. It is worthwhile mentioning that the conventional vector dominance picture with energy-dependent widths in the vector meson propagators can be shown to be in contradiction to the one-loop result of chiral perturbation theory (ChPT) [13], the effective field theory of the strong interactions. The present approach, on the other hand, satisfies theoretical constraints such as anomalous Ward identities, electromagnetic gauge invariance, exact two-body unitarity and matches in the low-energy limit to one-loop ChPT. Resonances are not taken into account explicitly, but are rather generated dynamically through the iteration of meson-meson interactions.

This work is organized as follows. In the next section we present the general structure of the amplitude, while in Sec. 3 the one-loop result of these decays within ChPT is derived. Some details of the chiral unitary approach are presented in Sec. 4 and the results are discussed in Sec. 5. We summarize our findings in Sec. 6. The full list of relevant $\mathcal{O}(p^6)$ counter terms is relegated to the appendix.

2 General structure of the amplitude

The decays $\eta^{(\prime)} \rightarrow \pi^+ \pi^- l^+ l^-$ (l^\pm represents either e^\pm or μ^\pm) are depicted in Fig. 1, where we also introduce the four-momenta of the particles. The invariant matrix element of the decay has the generic form

$$i\mathcal{M} = -ie \epsilon^{\mu\nu\alpha\beta} k_\mu p_\alpha^+ p_\beta^- A(s_{+-}, s_{+\gamma}, s_{-\gamma}) \frac{-ig_{\nu\rho}}{k^2} \bar{u}(q^-, \sigma) (-ie\gamma^\rho) v(q^+, \sigma') , \quad (1)$$

with spin indices σ, σ' and $A(s_{+-}, s_{+\gamma}, s_{-\gamma})$ summarizing all contributions to $\eta^{(\prime)} \rightarrow \pi^+ \pi^- \gamma^*$ (represented by the blob in Fig. 1). The Mandelstam variables $s_{+-}, s_{+\gamma}, s_{-\gamma}$ are defined as follows:

$$s_{+-} = (p^+ + p^-)^2 , \quad s_{+\gamma} = (p^+ + k)^2 , \quad s_{-\gamma} = (p^- + k)^2 . \quad (2)$$

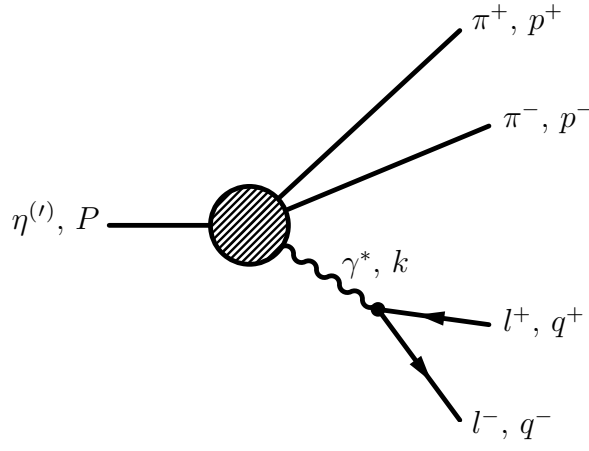


Figure 1: General structure of the process $\eta^{(l)}(P) \rightarrow \pi^+(p^+) \pi^-(p^-) l^+(q^+) l^-(q^-)$. The blob symbolizes the amplitude $\mathcal{A}(\eta^{(l)} \rightarrow \pi^+ \pi^- \gamma^*)$. The four-momentum of the intermediate photon is denoted by $k = P - p^+ - p^- = q^+ + q^-$ with $k^2 > 0$.

As a consequence of C invariance $A(s_{+-}, s_{+\gamma}, s_{-\gamma})$ is symmetric under the exchange $s_{+\gamma} \leftrightarrow s_{-\gamma}$. Clearly, the decay $\eta^{(l)} \rightarrow \pi^+ \pi^- l^+ l^-$ proceeds via the two-step mechanism $\eta^{(l)} \rightarrow \pi^+ \pi^- \gamma^*$ followed by $\gamma^* \rightarrow l^+ l^-$. Defining (in accordance with [14]) the n -body phase space element

$$d\Phi_n(P; p_1, \dots, p_n) = \delta^{(4)}\left(P - \sum_{i=1}^n p_i\right) \prod_{i=1}^n \frac{d^3 p_i}{(2\pi)^3 2E_i} \quad (3)$$

and making use of the factorization

$$d\Phi_4(P; q^+, q^-, p^+, p^-) = d\Phi_3(P; k, p^+, p^-) d\Phi_2(k; q^+, q^-) (2\pi)^3 dk^2 \quad (4)$$

one finds the following relation between the differential decay width of $\eta^{(l)} \rightarrow \pi^+ \pi^- l^+ l^-$ and the differential widths of the two sub-processes $\eta^{(l)} \rightarrow \pi^+ \pi^- \gamma^*$ and $\gamma^* \rightarrow l^+ l^-$, see *e.g.* [15]:

$$d\Gamma(\eta^{(l)} \rightarrow \pi^+ \pi^- l^+ l^-) = d\Gamma(\eta^{(l)} \rightarrow \pi^+ \pi^- \gamma^*) d\Gamma(\gamma^* \rightarrow l^+ l^-) \frac{1}{\pi} \frac{1}{k^2 \sqrt{k^2}} dk^2. \quad (5)$$

After integration over the dilepton phase space (PS ll) one arrives at

$$\int_{\text{PS}ll} d\Gamma(\eta^{(l)} \rightarrow \pi^+ \pi^- l^+ l^-) = d\Gamma(\eta^{(l)} \rightarrow \pi^+ \pi^- \gamma^*) \Gamma(\gamma^* \rightarrow l^+ l^-) \frac{1}{\pi} \frac{1}{k^2 \sqrt{k^2}} dk^2 \quad (6)$$

with

$$\Gamma(\gamma^* \rightarrow l^+ l^-) = \frac{\alpha}{3} \sqrt{k^2} \left(1 + \frac{2m_l^2}{k^2}\right) \sqrt{1 - \frac{4m_l^2}{k^2}}, \quad \alpha = \frac{e^2}{4\pi}. \quad (7)$$

The task of the current work is to calculate $A(s_{+-}, s_{+\gamma}, s_{-\gamma})$ (or, equivalently, the amplitude $\mathcal{A}(\eta^{(l)} \rightarrow \pi^+ \pi^- \gamma^*)$) within a chiral unitary approach.

3 One-loop calculation

In this section we present the result of the full one-loop calculation of the amplitude for $\eta^{(l)} \rightarrow \pi^+ \pi^- \gamma^*$ in U(3) ChPT generalizing the one-loop result of [12] for the decay amplitude $\eta^{(l)} \rightarrow$

$\pi^+\pi^-\gamma$. Here we will restrict ourselves to compiling the necessary formulae and outlining the basic steps of the calculation. For details we refer the reader to [12].

The amplitude $\mathcal{A}(\eta^{(\prime)} \rightarrow \pi^+\pi^-\gamma^*)$ involves the totally antisymmetric tensor $\epsilon^{\mu\nu\alpha\beta}$ and is thus of unnatural parity. At leading chiral order, the pure SU(3) process $\eta_8 \rightarrow \pi^+\pi^-\gamma^*$ is determined by the chiral anomaly of the underlying QCD Lagrangian. Within ChPT the chiral QCD anomalies are accounted for by the Wess-Zumino-Witten (WZW) action [16–20]

$$S_{WZW} = -\frac{i}{80\pi^2} \int_{M_5} d^5x \epsilon^{ijklm} \langle U^\dagger \partial_i U U^\dagger \partial_j U U^\dagger \partial_k U U^\dagger \partial_l U U^\dagger \partial_m U \rangle \quad (8)$$

$$+ \frac{e}{16\pi^2} \int d^4x \epsilon^{\mu\nu\alpha\beta} A_\mu \langle U \partial_\nu U^\dagger U \partial_\alpha U^\dagger U \partial_\beta U^\dagger Q - U^\dagger \partial_\nu U U^\dagger \partial_\alpha U U^\dagger \partial_\beta U Q \rangle ,$$

where we have displayed only the pieces of the action relevant for the present calculation. The octet of Goldstone bosons (π, K, η_8) and the singlet field η_0 are collected in the matrix valued field ϕ which enters into $U = \exp\{i\sqrt{2}\phi/f\}$, where f is the pseudoscalar decay constant in the chiral limit. The expression $\langle \dots \rangle$ denotes the trace in flavor space, A_μ is the photon field, and $Q = \frac{1}{3}\text{diag}(2, -1, -1)$ represents the charge matrix of the light quarks. The integration in the first line of Eq. (8) spans over a five-dimensional manifold M_5 , whose boundary is Minkowskian space, and the U fields in this integral are functions on M_5 . The additional fifth coordinate is defined to be timelike and the convention for the totally antisymmetric tensor is $\epsilon^{01234} = +1$, see [17, 19, 20] for further details.

The inclusion of the singlet field η_0 and, consequently, the extension of SU(3) ChPT to the U(3) framework introduces additional, non-anomalous terms of unnatural parity at chiral order $\mathcal{O}(p^4)$. The only term relevant for this work at $\mathcal{O}(p^4)$ reads

$$\mathcal{L}_{ct}^{(4)} = -ie \epsilon^{\mu\nu\alpha\beta} \partial_\mu A_\nu W_3 \langle \partial_\alpha U \partial_\beta U^\dagger Q + \partial_\alpha U^\dagger \partial_\beta U Q \rangle , \quad (9)$$

where W_3 is a function of η_0 , $W_3(\eta_0/f)$, which can be expanded in the singlet field with coefficients $w_3^{(j)}$ that are not fixed by chiral symmetry. Parity conservation implies that W_3 is an odd function of η_0 .

In addition to the leading-order tree level contributions derived from Eqs. (8) and (9) there are next-to-leading order chiral corrections from one-loop graphs, decay constants, η - η' mixing, and wave function renormalization which involve terms both from the $\mathcal{O}(p^0) + \mathcal{O}(p^2)$ Lagrangian and the $\mathcal{O}(p^4)$ Lagrangian of natural parity with couplings $v_i^{(j)}$ and $\beta_i^{(j)}$, respectively. The full list of terms up to $\mathcal{O}(p^4)$ can be found, *e.g.*, in [21]. Finally, the process $\eta^{(\prime)} \rightarrow \pi^+\pi^-\gamma^*$ receives contributions from counter terms of the unnatural parity $\mathcal{O}(p^6)$ Lagrangian, which also absorb the divergences of the one-loop integrals.

Fig. 2 shows the pertinent one-loop diagrams contributing to $\eta^{(\prime)} \rightarrow \pi^+\pi^-\gamma^*$ (except for contributions from wave function renormalization). The full one-loop result reads

$$\mathcal{A}^{(1-loop)}(\eta^{(\prime)} \rightarrow \pi^+\pi^-\gamma^*) = -ek_\mu \epsilon_\nu p_\alpha^+ p_\beta^- \epsilon^{\mu\nu\alpha\beta} \frac{1}{4\pi^2 F_{\eta^{(\prime)}} F_\pi^2} \beta_{\eta^{(\prime)}}^{(1-loop)} , \quad (10)$$

where ϵ_ν is the polarization vector of the virtual photon and the coefficients $\beta_{\eta^{(\prime)}}^{(1-loop)}$ are given

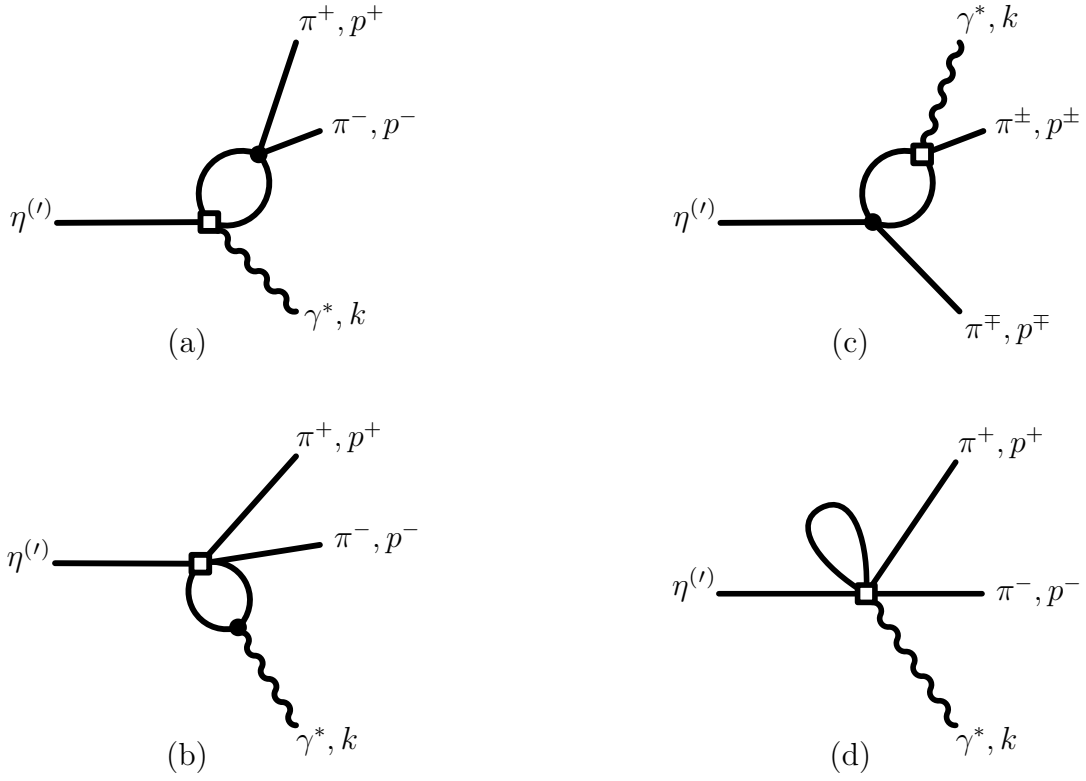


Figure 2: One loop diagrams contributing to the process $\eta^{(\prime)} \rightarrow \pi^+ \pi^- \gamma^*$. The empty squares denote vertices from the $\mathcal{O}(p^4)$ Lagrangian of unnatural parity, whereas vertices from the leading order Lagrangian of natural parity are indicated by a filled circle.

by

$$\begin{aligned}
\beta_{\eta}^{(1-loop)} &= \frac{1}{\sqrt{3}} \left\{ 1 + \frac{1}{F_{\eta}^2} \left[4\sqrt{\frac{2}{3}} \left(\sqrt{\frac{2}{3}} - 16\pi^2 w_3^{(1)r} \right) (m_K^2 - m_{\pi}^2) \frac{\tilde{v}_2^{(1)}}{v_0^{(2)}} \right. \right. \\
&\quad \left. \left. - 3\Delta(m_{\pi}^2) - 3\Delta(m_K^2) + 3I(m_K^2, m_K^2, k^2) + I(m_{\pi}^2, m_{\pi}^2, s_{+-}) + 2I(m_K^2, m_K^2, s_{+-}) \right] \right. \\
&\quad \left. + 64\pi^2 (\bar{w}_{\eta}^{(m)} + \bar{w}_{\eta}^{(s)} s_{+-} + \bar{w}_{\eta}^{(k)} k^2) \right\}, \\
\beta_{\eta'}^{(1-loop)} &= \left(\sqrt{\frac{2}{3}} - 16\pi^2 w_3^{(1)r} \right) \left\{ 1 + \frac{1}{F_{\eta'}^2} \left[4(2m_K^2 + m_{\pi}^2) \left(\beta_{46}^{(0)} + 3\beta_{47}^{(0)} - \beta_{53}^{(0)} - \sqrt{\frac{3}{2}} \beta_{52}^{(1)} \right) \right. \right. \\
&\quad \left. \left. - 3\Delta(m_{\pi}^2) - \frac{3}{2}\Delta(m_K^2) + I(m_{\pi}^2, m_{\pi}^2, s_{+-}) + \frac{1}{2}I(m_K^2, m_K^2, s_{+-}) \right. \right. \\
&\quad \left. \left. - 4v_1^{(2)} (I'(m_{\pi}^2, m_{\eta'}^2, s_{+\gamma}) + I'(m_{\pi}^2, m_{\eta'}^2, s_{-\gamma})) \right] \right\} \\
&\quad + \frac{4}{3} \sqrt{\frac{2}{3}} (m_K^2 - m_{\pi}^2) \left(4 \frac{\beta_{5,18}}{F_{\eta'}^2} - \frac{\tilde{v}_2^{(1)}}{v_0^{(2)}} \right) + 32\pi^2 \sqrt{\frac{2}{3}} (\bar{w}_{\eta'}^{(m)} + \bar{w}_{\eta'}^{(s)} s_{+-} + \bar{w}_{\eta'}^{(k)} k^2).
\end{aligned} \tag{11}$$

In this expression we have perturbatively substituted the pseudoscalar decay constant in the chiral limit, f , by the physical decay constants F_{π} , F_{η} , $F_{\eta'}$ of π , η , η' , respectively, and employed the abbreviations

$$\tilde{v}_2^{(1)} = \frac{1}{4}f^2 - \frac{1}{2}\sqrt{6}v_3^{(1)}, \quad \beta_{5,18} = \beta_5^{(0)} + \frac{3}{2}\beta_{18}^{(0)}. \tag{12}$$

The loop integrals are calculated using dimensional regularization and the pertinent regularization scale is denoted by μ . The finite parts of the loop integrals are given by

$$\Delta(m^2) = \left(\int \frac{d^d l}{(2\pi)^d} \frac{i}{l^2 - m^2 + i\varepsilon} \right)_{finite} = \frac{m^2}{16\pi^2} \ln \frac{m^2}{\mu^2} \tag{13}$$

and

$$\begin{aligned}
I(m^2, \bar{m}^2, p^2) &= \frac{1}{6p^2} \{ - (p^2 - (m - \bar{m})^2)(p^2 - (m + \bar{m})^2) G_{m\bar{m}}(p^2) \\
&\quad + (p^2 + m^2 - \bar{m}^2) \Delta(m^2) + (p^2 - m^2 + \bar{m}^2) \Delta(\bar{m}^2) \} \\
&\quad + \frac{1}{144\pi^2} (p^2 - 3m^2 - 3\bar{m}^2),
\end{aligned} \tag{14}$$

where $G_{m\bar{m}}$ is the finite part of the scalar one-loop integral

$$\begin{aligned}
G_{m\bar{m}}(p^2) &= \left(\int \frac{d^d l}{(2\pi)^d} \frac{i}{(l^2 - m^2 + i\epsilon)((l-p)^2 - \bar{m}^2 + i\epsilon)} \right)_{finite} \\
&= \frac{1}{16\pi^2} \left[-1 + \ln \frac{m\bar{m}}{\mu^2} + \frac{m^2 - \bar{m}^2}{p^2} \ln \frac{m}{\bar{m}} \right. \\
&\quad \left. - \frac{2\sqrt{\lambda_{m\bar{m}}(p^2)}}{p^2} \operatorname{artanh} \frac{\sqrt{\lambda_{m\bar{m}}(p^2)}}{(m + \bar{m})^2 - p^2} \right], \tag{15}
\end{aligned}$$

$$\lambda_{m\bar{m}}(p^2) = ((m - \bar{m})^2 - p^2)((m + \bar{m})^2 - p^2).$$

The integral I' is defined via the subtraction

$$I'(m^2, \bar{m}^2, p^2) = I(m^2, \bar{m}^2, p^2) - I(0, \bar{m}^2, 0) \tag{16}$$

which guarantees chiral power counting for loops involving the η' . Since the mass of this heavy degree of freedom does not vanish in the chiral limit, its presence can in principle spoil the chiral counting scheme. However, it has been shown in [12] that all power-counting violating contributions to the process $\eta^{(\prime)} \rightarrow \pi^+ \pi^- \gamma^*$ can be absorbed into a redefinition of the low-energy constant $w_3^{(1)}$; the renormalized value is denoted by $w_3^{(1)r}$.

The last terms in the expressions for $\beta_{\eta^{(\prime)}}^{(1-loop)}$ in Eq. (11) summarize the contributions of counter terms from the $\mathcal{O}(p^6)$ Lagrangian of unnatural parity. The relations between the constants $\bar{w}_{\eta^{(\prime)}}^{(m)}$, $\bar{w}_{\eta^{(\prime)}}^{(s)}$, $\bar{w}_{\eta^{(\prime)}}^{(k)}$ and the numerous couplings of the Lagrangian of sixth chiral order are given in the appendix.

4 Chiral unitary approach

From the analysis of various η and η' decays, see *e.g.* [9, 11, 12], it has become clear that resonances and unitarity corrections due to final-state interactions are a necessary ingredient for the realistic description of these processes. One example is the pronounced peak structure caused by the $\rho(770)$ resonance in the $\pi^+ \pi^-$ spectrum of $\eta' \rightarrow \pi^+ \pi^- \gamma$ [22, 23] (see also Fig. 5). Hence, a conventional loop-wise expansion within ChPT is usually not sufficient to successfully describe η and—in particular— η' decays.

Instead of taking resonances into account explicitly, as *e.g.* in [15, 24, 25], we prefer to work within a chiral unitary approach which combines ChPT and a non-perturbative resummation based on the Bethe-Salpeter equation (BSE). In this framework the resulting multi-channel T -matrix of meson-meson scattering satisfies exact two-body unitarity. Our approach has the further advantages that electromagnetic gauge invariance is automatically maintained, anomalous chiral Ward identities are satisfied, and the result matches to one-loop ChPT in the low-energy limit. Resonances are generated dynamically and are identified with poles of the T -matrix in the complex energy plane.

Since this approach has already been discussed in detail in [11, 12] we will only recapitulate the basic formulae here. From the effective Lagrangian up to fourth chiral order one extracts

the partial wave interaction kernel A_ℓ for meson-meson scattering which is then iterated in the BSE

$$T_\ell = A_\ell - A_\ell \tilde{G} T_\ell . \quad (17)$$

The diagonal matrix \tilde{G} collects the modified scalar loop integrals

$$\tilde{G}_{m\bar{m}} = G_{m\bar{m}}(\mu) + a_{m\bar{m}}(\mu) , \quad (18)$$

where we have added a subtraction constant $a_{m\bar{m}}(\mu)$ to the integral $G_{m\bar{m}}$ defined in Eq. (15) which varies with the scale μ in such a way that $\tilde{G}_{m\bar{m}}$ is scale-independent [26]. After adjusting the occurring parameters the partial-wave T -matrix resulting from the BSE accurately describes the experimental phase shifts in both the s - and p -wave channels [11, 27].

The implementation of non-perturbative meson-meson rescattering generated by the BSE in the amplitude $\mathcal{A}(\eta^{(\prime)} \rightarrow \pi^+ \pi^- \gamma^*)$ is accomplished in the same way as in [12]. The pertinent graphs are shown in Fig. 3 and the corresponding amplitude is added to the one-loop result presented in the previous section. We point out that a possible double counting of one-loop contributions, which in principle arises since the diagrams (a) and (c) in Fig. 3 incorporate also one-loop terms, has been properly taken care of. The amplitude corresponding to the diagram in Fig. 3a is given by

$$\begin{aligned} \mathcal{A}^{(CCa)}(\eta^{(\prime)} \rightarrow \pi^+ \pi^- \gamma^*) &= -ek_\mu \epsilon_\nu p_\alpha^+ p_\beta^- \epsilon^{\mu\nu\alpha\beta} \frac{1}{4\pi^2 F_\pi^3} \\ &\times \sum_a' \gamma_{\eta^{(\prime)}}^{(CCa),a} \tilde{I}(m_a^2, m_a^2, s_{+-}, C_a) \hat{T}_p^{(a \rightarrow \pi^\pm)}(s_{+-}) \end{aligned} \quad (19)$$

with

$$\begin{aligned} \gamma_{\eta}^{(CCa),\pi^\pm} &= \gamma_{\eta}^{(CCa),K^\pm} = \frac{1}{6} \left[\sqrt{3} + \frac{4\sqrt{2}}{3} (m_K^2 - m_\pi^2) \frac{\tilde{v}_2^{(1)}}{v_0^{(2)}} (\sqrt{6} - 48\pi^2 w_3^{(1)r}) \right] , \\ \gamma_{\eta}^{(CCa),K^0 \bar{K}^0} &= -\frac{\sqrt{3}}{2} , \\ \gamma_{\eta'}^{(CCa),\pi^\pm} &= \gamma_{\eta'}^{(CCa),K^\pm} \\ &= \frac{1}{6} \left[\sqrt{6} - 48\pi^2 w_3^{(1)r} + \frac{4\sqrt{6}}{3} (m_K^2 - m_\pi^2) \left(4 \frac{\beta_{5,18}}{F_{\eta'}^2} - \frac{\tilde{v}_2^{(1)}}{v_0^{(2)}} \right) \right] , \\ \gamma_{\eta'}^{(CCa),K^0 \bar{K}^0} &= -2\sqrt{\frac{2}{3}} (m_K^2 - m_\pi^2) \left(4 \frac{\beta_{5,18}}{F_{\eta'}^2} - \frac{\tilde{v}_2^{(1)}}{v_0^{(2)}} \right) . \end{aligned} \quad (20)$$

The symbol \sum' in Eq. (19) denotes summation over the meson pairs $\pi^+ \pi^-$, $K^+ K^-$ and $K^0 \bar{K}^0$ and $\hat{T}_p^{(a \rightarrow b)}$ represents the p -wave part of T -matrix for scattering of a meson pair a into a meson pair b . It differs from the solution of the BSE, T_p , only by kinematical factors, see [11] for details. The loop integral \tilde{I} is given by

$$\tilde{I}(m^2, \bar{m}^2, p^2, C_{m\bar{m}}) = I(m^2, \bar{m}^2, p^2) + (p^2 - 3m^2 - 3\bar{m}^2) C_{m\bar{m}} \quad (21)$$

with I defined in Eq. (14). In order to keep the notation compact we set

$$C_\pi \equiv C_{m_\pi m_\pi} , \quad C_K \equiv C_{m_K m_K} , \quad C_{\pi\eta} \equiv C_{m_\pi m_\eta} , \quad C_{\pi\eta'} \equiv C_{m_\pi m_{\eta'}} . \quad (22)$$

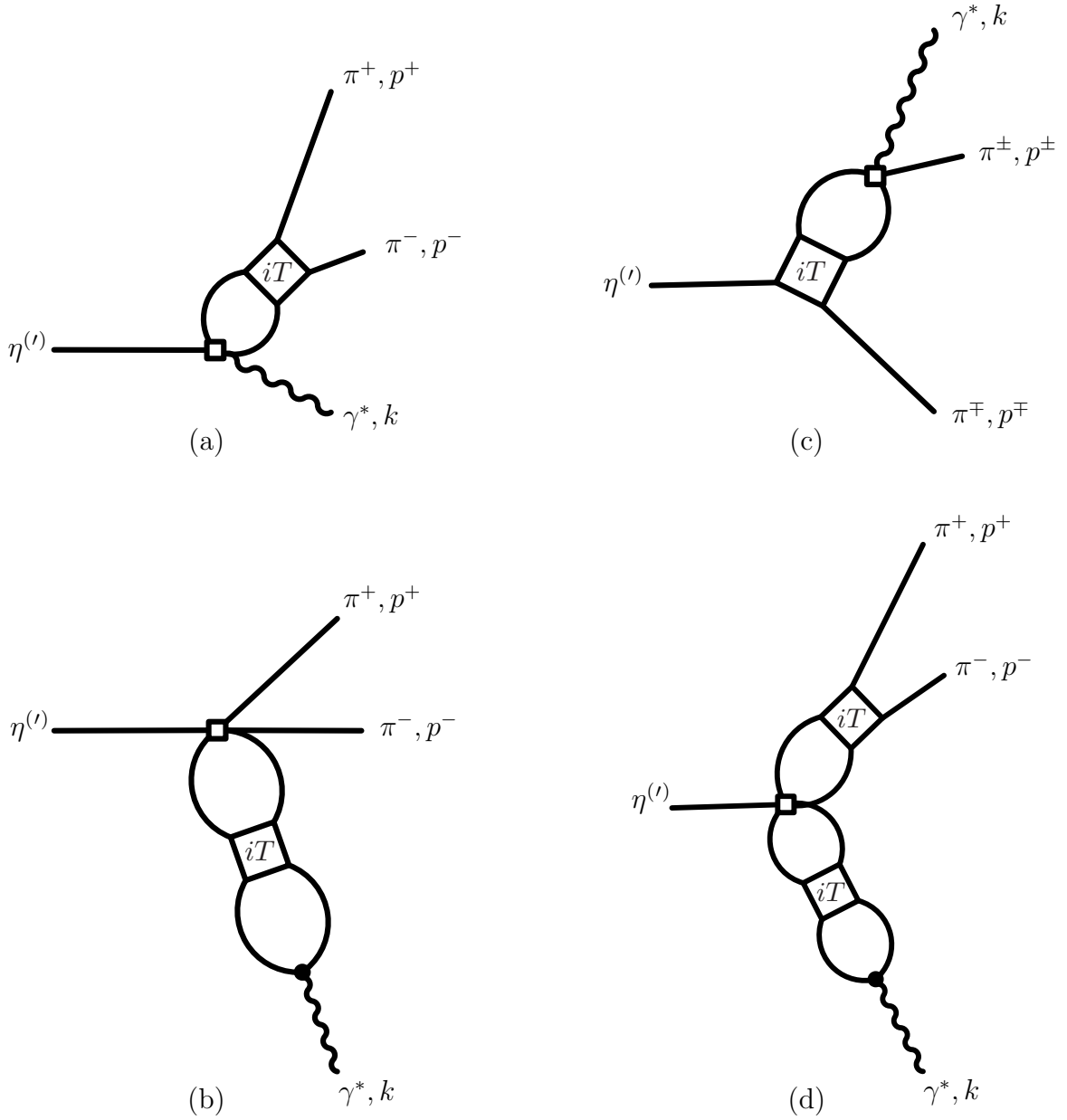


Figure 3: Set of meson-meson rescattering diagrams which contribute to the process $\eta^{(\prime)} \rightarrow \pi^+ \pi^- \gamma^*$ and are taken into account in this approach. The empty squares denote vertices from the $\mathcal{O}(p^4)$ Lagrangian of unnatural parity whereas vertices from the leading order Lagrangian of natural parity are indicated by a filled circle.

Note that the definition of \tilde{I} slightly differs from that of \tilde{I}_1 in [12], where the constant C was chosen to be the coefficient of p^2 instead of $(p^2 - 3m^2 - 3\bar{m}^2)$. Here, we prefer to work with the decomposition in Eq. (21) since then the regularization scale dependence of I can be completely absorbed into the constant C . We point out that in an effective field theory framework one is free to arbitrarily modify the analytic piece of an amplitude by adjusting unconstrained counter terms.

The diagram in Fig. 3b produces the amplitude

$$\begin{aligned} \mathcal{A}^{(CCb)}(\eta^{(\prime)} \rightarrow \pi^+ \pi^- \gamma^*) &= -ek_\mu \epsilon_\nu p_\alpha^+ p_\beta^- \epsilon^{\mu\nu\alpha\beta} \frac{1}{4\pi^2 F_\pi^5} \sum_a' \gamma_{\eta^{(\prime)}}^{(CCb),a} \tilde{I}(m_K^2, m_K^2, k^2, C_K) \\ &\times \left[\hat{T}_p^{(a \rightarrow \pi^\pm)}(k^2) \tilde{I}(m_\pi^2, m_\pi^2, k^2, C_\pi) + \hat{T}_p^{(a \rightarrow K^\pm)}(k^2) \tilde{I}(m_K^2, m_K^2, k^2, C_K) \right], \end{aligned} \quad (23)$$

where the coefficients $\gamma_{\eta^{(\prime)}}^{(CCb),a}$ are given by

$$\begin{aligned} \gamma_\eta^{(CCb),\pi^\pm} &= \gamma_{\eta'}^{(CCb),\pi^\pm} = 0, \quad \gamma_\eta^{(CCb),K^\pm} = -\gamma_\eta^{(CCb),K^0 \bar{K}^0} = \frac{\sqrt{3}}{2}, \\ \gamma_{\eta'}^{(CCb),K^\pm} &= -\gamma_{\eta'}^{(CCb),K^0 \bar{K}^0} = 2\sqrt{\frac{2}{3}}(m_K^2 - m_\pi^2) \left(4\frac{\beta_{5,18}}{F_{\eta'}^2} - \frac{\tilde{v}_2^{(1)}}{v_0^{(2)}} \right). \end{aligned} \quad (24)$$

The amplitude corresponding to graph (c) in Fig. 3 is given by

$$\begin{aligned} \mathcal{A}^{(CCc)}(\eta^{(\prime)} \rightarrow \pi^+ \pi^- \gamma^*) &= -ek_\mu \epsilon_\nu p_\alpha^+ p_\beta^- \epsilon^{\mu\nu\alpha\beta} \frac{1}{4\pi^2 F_\pi^3} \\ &\times \frac{1}{2} \left\{ \frac{1}{\sqrt{3}} \left[\tilde{I}(m_\pi^2, m_\eta^2, s_{+\gamma}, C_{\pi\eta}) \hat{T}_p^{(\eta^{(\prime)} \pi^+ \rightarrow \eta \pi^+)}(s_{+\gamma}) + \tilde{I}(m_\pi^2, m_\eta^2, s_{-\gamma}, C_{\pi\eta}) \hat{T}_p^{(\eta^{(\prime)} \pi^- \rightarrow \eta \pi^-)}(s_{-\gamma}) \right] \right. \\ &\quad + \left(\sqrt{\frac{2}{3}} - 16\pi^2 w_3^{(1)r} \right) \left[\tilde{I}'(m_\pi^2, m_{\eta'}^2, s_{+\gamma}, C_{\pi\eta'}) \hat{T}_p^{(\eta^{(\prime)} \pi^+ \rightarrow \eta' \pi^+)}(s_{+\gamma}) \right. \\ &\quad \left. \left. + \tilde{I}'(m_\pi^2, m_{\eta'}^2, s_{-\gamma}, C_{\pi\eta'}) \hat{T}_p^{(\eta^{(\prime)} \pi^- \rightarrow \eta' \pi^-)}(s_{-\gamma}) \right] \right\}, \end{aligned} \quad (25)$$

where the integral \tilde{I}' is defined analogously to I' , Eq. (16), by

$$\tilde{I}'(m^2, \bar{m}^2, p^2, C_{m\bar{m}}) = \tilde{I}(m^2, \bar{m}^2, p^2, C_{m\bar{m}}) - \tilde{I}(0, \bar{m}^2, 0, C_{m\bar{m}}). \quad (26)$$

Finally, we include the diagram with two insertions of iterated meson-meson rescattering, Fig. 3d. The corresponding amplitude reads

$$\begin{aligned} \mathcal{A}^{(2CC)}(\eta^{(\prime)} \rightarrow \pi^+ \pi^- \gamma^*) &= -ek_\mu \epsilon_\nu p_\alpha^+ p_\beta^- \epsilon^{\mu\nu\alpha\beta} \frac{1}{4\pi^2 F_\pi^5} \sum_{a,b}' \gamma_{\eta^{(\prime)}}^{(2CC),a,b} \\ &\times \tilde{I}(m_a^2, m_a^2, s_{+-}, C_a) \hat{T}_p^{(a \rightarrow \pi^\pm)}(s_{+-}) \tilde{I}(m_b^2, m_b^2, k^2, C_b) \\ &\times \left[\hat{T}_p^{(b \rightarrow \pi^\pm)}(k^2) \tilde{I}(m_\pi^2, m_\pi^2, k^2, C_\pi) + \hat{T}_p^{(b \rightarrow K^\pm)}(k^2) \tilde{I}(m_K^2, m_K^2, k^2, C_K) \right] \end{aligned} \quad (27)$$

with coefficients $\gamma_{\eta^{(\prime)}}^{(2\,CC),a,b}$ symmetric under the interchange $a \leftrightarrow b$

$$\begin{aligned}\gamma_{\eta}^{(2\,CC),\pi^{\pm},K^{\pm}} &= -\gamma_{\eta}^{(2\,CC),\pi^{\pm},K^0\bar{K}^0} = -\frac{1}{2}\gamma_{\eta}^{(2\,CC),K^{\pm},K^0\bar{K}^0} = \frac{\sqrt{3}}{4}, \\ \gamma_{\eta'}^{(2\,CC),\pi^{\pm},K^{\pm}} &= -\gamma_{\eta'}^{(2\,CC),\pi^{\pm},K^0\bar{K}^0} = -\frac{1}{2}\gamma_{\eta'}^{(2\,CC),K^{\pm},K^0\bar{K}^0} \\ &= \sqrt{\frac{2}{3}}(m_K^2 - m_{\pi}^2) \left(4\frac{\beta_{5,18}}{F_{\eta'}^2} - \frac{\tilde{v}_2^{(1)}}{v_0^{(2)}} \right)\end{aligned}\tag{28}$$

and zero otherwise.

5 Results

The chiral unitary approach discussed in this work involves several free parameters which must be fixed from experiment. On the one hand, there are the coupling constants of the chiral Lagrangian which can be grouped into coefficients of the natural parity part of $\mathcal{O}(p^0) + \mathcal{O}(p^2)$ and $\mathcal{O}(p^4)$, $v_i^{(j)}$ and $\beta_i^{(j)}$, respectively, and coefficients of the unnatural parity part of $\mathcal{O}(p^4)$ and $\mathcal{O}(p^6)$, $w_i^{(j)}$ and $\bar{w}_i^{(j)}$, respectively. On the other hand, there are the subtraction constants a and C in the loop integrals whose values correspond to a specific choice of the infinitely many higher order counter terms neglected in this non-perturbative approach. For consistency with previous work [9] the coupling constants of the Lagrangian of natural parity and the subtraction constant $a_{\pi\pi}^{(I=J=1)}$ in the isospin one p -wave $\pi\pi$ channel are fixed by a fit to the hadronic decay modes of η and η' , $\eta^{(\prime)} \rightarrow 3\pi$ and $\eta' \rightarrow \eta\pi\pi$, and the phase shifts of meson-meson scattering. This fit is in very good agreement with the bulk of the available experimental data. The subtraction constants in the other meson-meson channels do not have any relevant impact on the discussed data and can be set to zero for our purposes. The pseudoscalar decay constants are set to $F_{\pi} = 92.4\text{ MeV}$, $F_{\eta} = 1.3F_{\pi}$, and $F_{\eta'} = 1.1F_{\pi}$ [11, 12].

The couplings of the unnatural parity part of the Lagrangian and the subtraction constants C are taken as free parameters, which are constrained by fitting to the available spectra and widths of the decays $\eta^{(\prime)} \rightarrow \pi^+\pi^-\gamma$. It turns out, however, that in order to achieve agreement with the experimental data, only the subtraction constant in the pion loops, C_{π} , is required to have a non-vanishing value, and we set all other subtraction constants to zero for simplicity. To further reduce the number of parameters and for consistency with previous investigations [11, 12], we also set the renormalized coupling constant $w_3^{(1)r}$ of the unnatural parity Lagrangian at $\mathcal{O}(p^4)$ to zero. We have confirmed that small variations in $w_3^{(1)r}$ do not alter our conclusions. Finally, the combinations of $\mathcal{O}(p^6)$ unnatural parity couplings denoted by $\bar{w}_{\eta^{(\prime)}}^{(k)}$, which do not contribute to processes with on-shell photons and thus cannot be constrained by $\eta^{(\prime)} \rightarrow \pi^+\pi^-\gamma$, will be neglected for the time being. Changes of the results due to non-zero values of these coefficients will be discussed at the end of this section. To summarize, there are five parameters, C_{π} , $\bar{w}_{\eta}^{(m)}$, $\bar{w}_{\eta}^{(s)}$, $\bar{w}_{\eta'}^{(m)}$, and $\bar{w}_{\eta'}^{(s)}$ which are constrained by fitting the decays $\eta^{(\prime)} \rightarrow \pi^+\pi^-\gamma$. Afterwards, we can predict the spectra and widths of $\eta^{(\prime)} \rightarrow \pi^+\pi^-l^+l^-$ within this approach.

The data of $\eta^{(\prime)} \rightarrow \pi^+\pi^-\gamma$ involve the partial decay widths [14] and the di-pion spectra from [22, 23, 28, 29]. In order to perform a global least-squares fit to these different data sets we

employ the following definition for the χ^2 -function:

$$\frac{\chi^2}{\text{d.o.f.}} = \frac{\sum_i n_i}{N(\sum_i n_i - p)} \sum_i \frac{\chi_i^2}{n_i}, \quad (29)$$

where N is the number of observables and p the number of free parameters in the approach. The quantity χ_i^2 is the standard χ^2 -value computed for the i -th data set with n_i data points. The above definition was introduced in [30] to equally weight each data set and to prevent, *e.g.*, sets with only one data point (such as decay widths) from being dominated by sets with many data points (such as spectra).

In order to quantify an error for our analysis we employ the condition [14]

$$\frac{\chi^2}{\text{d.o.f.}} \leq \frac{\chi_{\min}^2}{\text{d.o.f.}} + \frac{\Delta\chi^2}{\text{d.o.f.}} \quad (30)$$

where $\Delta\chi^2$ is derived from the p -value of the χ^2 probability distribution function. One finds that in the present investigation employing $\Delta\chi^2/\text{d.o.f.} = 1.08$ corresponds to the 1σ confidence region. Strictly speaking, this standard definition of a confidence region, Eq. (30), holds only if the fit is performed to just one observable and the fit function is linear in the fit parameters. Although both constraints are not fulfilled here, one can expect Eq. (30) to be a reasonable approximation in the vicinity of the minimum of the χ^2 -function, see also [31]. We have significantly improved our fitting routine compared to the previous investigation [12] and performed a large number of fits so that the 1σ confidence region is populated by about 1000 qualitatively different fits providing a realistic estimate of the theoretical uncertainty within this approach.

In Figs. 4 and 5 the result of the calculation is compared to the available experimental spectra which are given in terms of the photon energy for $\eta \rightarrow \pi^+\pi^-\gamma$ and in terms of the invariant mass of the $\pi^+\pi^-$ system for $\eta' \rightarrow \pi^+\pi^-\gamma$. The solid line corresponds to the best fit with an overall $\chi^2/\text{d.o.f.} = 2.23$, the error bands indicate the 1σ confidence level. For the η' decay the agreement with the two experimental spectra from [22, 23] is very good as already observed in [12]. The experimental situation for the η decay is not as consistent as for $\eta' \rightarrow \pi^+\pi^-\gamma$. First, both the spectra published in [28, 29] have not been corrected for the detection efficiency which is given separately in [28], but must be deduced in [29]. Also, in both experiments it is impossible to quantify the systematic error resulting from the correction of the detection efficiency which introduces an uncontrolled uncertainty in the data. Second, when taking into account the two data sets from [28] and [29] simultaneously in the fit, it turns out that they are not fully consistent, at least without knowledge of the complete systematic errors. As a consequence, the major part of the total $\chi^2/\text{d.o.f.}$ value is due to the disagreement between the two data sets. In fact, the best fit (solid line in Fig. 4) must be considered as a compromise of [28] and [29], so that under these circumstances a total $\chi^2/\text{d.o.f.}$ close to 1 cannot be achieved. If, however, only one of the two spectra is included in the fit, a total $\chi^2/\text{d.o.f.} \simeq 1$ can be obtained. In this context, further experimental investigations—such as [2]—with substantially improved accuracy should lead to a more consistent picture of the $\eta \rightarrow \pi^+\pi^-\gamma$ spectrum.

The numerical results for the branching ratios and decay widths of $\eta^{(\prime)} \rightarrow \pi^+\pi^-\gamma$, $\eta^{(\prime)} \rightarrow \pi^+\pi^-l^+l^-$ are shown in Table 1. The central values of our results correspond to the fit with minimal χ^2 , the error bars reflect the 1σ confidence region given within our approach. The agreement with the decay modes involving on-shell photons, which have been taken as input to

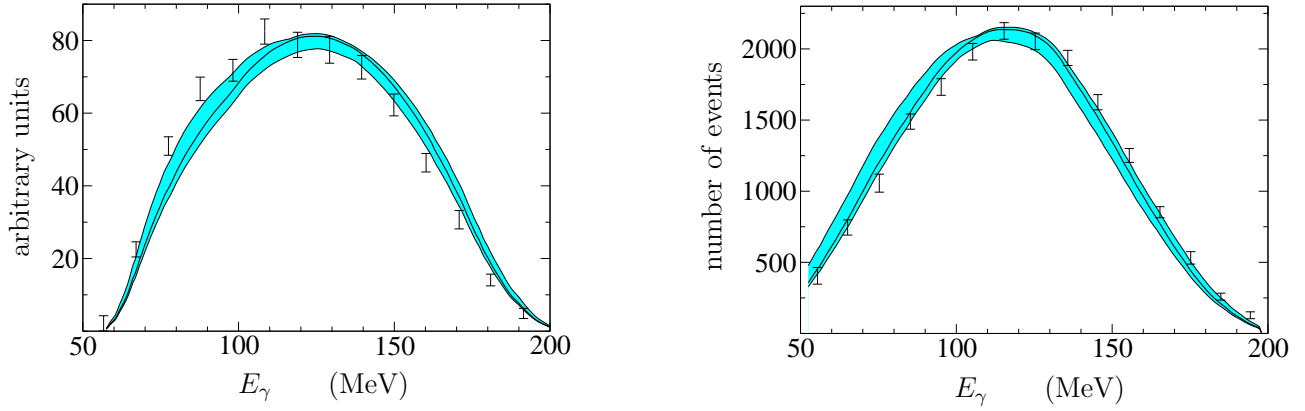


Figure 4: Photon spectrum of $\eta \rightarrow \pi^+\pi^-\gamma$ compared to experimental data from [28] (left) and [29] (right). The solid line corresponds to the fit with minimal χ^2 , the error band indicates the 1σ confidence region. For comparison with the experimental data points, the curves have been multiplied by the experimental detection efficiencies, hence the different shapes in the two plots.

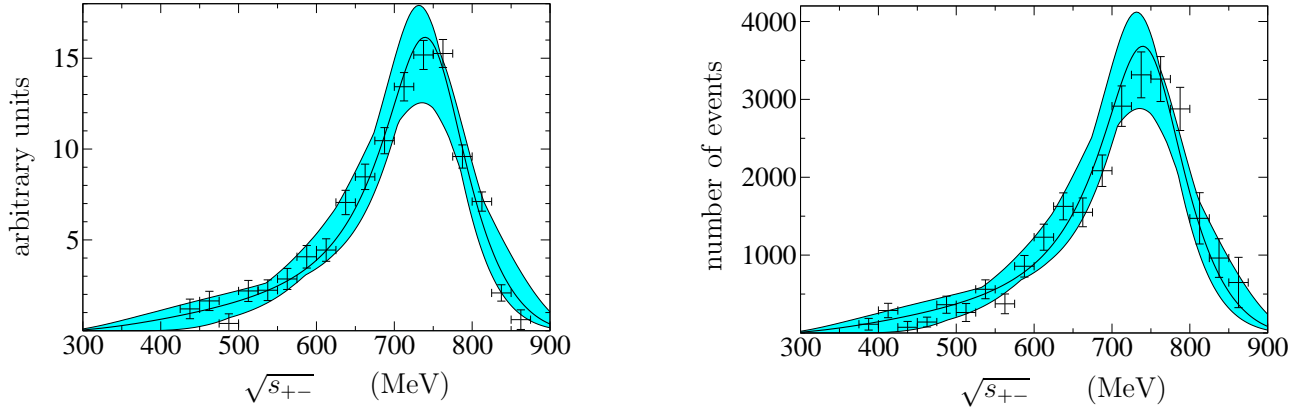


Figure 5: Invariant mass spectrum of the $\pi^+\pi^-$ system in $\eta' \rightarrow \pi^+\pi^-\gamma$ compared to experimental data from [22] (left) and [23] (right). The solid line corresponds to the fit with minimal χ^2 , the error band indicates the 1σ confidence region. All curves are normalized to the integral of the experimental histogram.

	this work	[24, 25]	[15]	experiment
$\text{BR}(\eta \rightarrow \pi^+\pi^-\gamma)$ (%)	$4.68^{+0.09}_{-0.09}$		6.9	4.69 ± 0.5 [14]
$\text{BR}(\eta' \rightarrow \pi^+\pi^-\gamma)$ (%)	$29.4^{+2.7}_{-4.3}$		25	29.4 ± 0.9 [14]
$\text{BR}(\eta \rightarrow \pi^+\pi^-e^+e^-)$ (10^{-4})	$2.99^{+0.06}_{-0.09}$		3.6	4.3 ± 1.7 [32]
$\text{BR}(\eta' \rightarrow \pi^+\pi^-e^+e^-)$ (10^{-3})	$2.13^{+0.17}_{-0.31}$		1.8	—
$\text{BR}(\eta \rightarrow \pi^+\pi^-\mu^+\mu^-)$ (10^{-9})	$7.5^{+1.8}_{-0.7}$		12	—
$\text{BR}(\eta' \rightarrow \pi^+\pi^-\mu^+\mu^-)$ (10^{-5})	$1.57^{+0.40}_{-0.47}$		2.0	—
$\Gamma(\eta \rightarrow \pi^+\pi^-\gamma)$ (eV)	$60.9^{+1.1}_{-1.2}$	62		60.8 ± 3.5 [14]
$\Gamma(\eta' \rightarrow \pi^+\pi^-\gamma)$ (keV)	60^{+6}_{-9}			60 ± 5 [14]
$\Gamma(\eta \rightarrow \pi^+\pi^-e^+e^-)$ (meV)	389^{+8}_{-11}	380		560 ± 260 [32]
$\Gamma(\eta' \rightarrow \pi^+\pi^-e^+e^-)$ (eV)	431^{+35}_{-62}			—
$\Gamma(\eta \rightarrow \pi^+\pi^-\mu^+\mu^-)$ (μeV)	$9.8^{+2.3}_{-0.9}$			—
$\Gamma(\eta' \rightarrow \pi^+\pi^-\mu^+\mu^-)$ (eV)	$3.2^{+0.9}_{-1.0}$			—

Table 1: Results for the branching ratios (BR) and widths (Γ) of the decay modes under consideration compared to experimental values and the theoretical analyses [24, 25] and [15]. See text for further details.

$\bar{w}_\eta^{(m)} \times 10^3$	$\bar{w}_{\eta'}^{(m)} \times 10^3$	$\bar{w}_\eta^{(s)} \times 10^3 \text{ GeV}^2$	$\bar{w}_{\eta'}^{(s)} \times 10^3 \text{ GeV}^2$	$C_\pi \times 10^2$
$-3.4^{+6.6}_{-2.0}$	$-20.1^{+35.1}_{-7.5}$	$1.2^{+2.6}_{-11.8}$	$-8.8^{+18.5}_{-23.8}$	$1.9^{+0.7}_{-3.6}$

Table 2: Numerical values of the fitted parameters at the regularization scale $\mu = 1 \text{ GeV}$. The central values correspond to the fit with minimal χ^2 , the error ranges are given by the 1σ confidence region.

the fit, is very good. The numerical values of the fit parameters, *i.e.* the counter terms $\bar{w}_{\eta^{(\prime)}}^{(m)}$, $\bar{w}_{\eta^{(\prime)}}^{(s)}$ and the subtraction constant C_π , are compiled in Table 2. Having fixed all parameters from data, we can make predictions for the decays into $\pi^+\pi^-$ and a lepton-antilepton pair. Up to now, the only branching ratio of this type which has been determined experimentally is $\eta \rightarrow \pi^+\pi^-e^+e^-$. We compare our result with the very recent experiment [32] which has improved precision compared to the PDG number [14] and we observe nice agreement.

Moreover, we can compare our results with those of [24, 25] and [15]. In [24, 25] a chiral Lagrangian with explicit vector mesons is used to calculate both the decay widths and spectra of $\eta \rightarrow \pi^+\pi^-\gamma$ and $\eta \rightarrow \pi^+\pi^-e^+e^-$. As shown in Table 1 and Figs. 6, 7 the agreement with our results is very good. However, it should be remarked that the results presented in [25] depend sensitively on the numerical values employed for the meson masses. Using the final expression Eq. (4) in [25] and inserting up-to-date meson mass values from [14], one computes $\Gamma(\eta \rightarrow \pi^+\pi^-e^+e^-) = 403 \text{ meV}$ instead of 380 meV as given in [25]. Also, the invariant mass spectra shown in Figs. 6, 7 are rescaled accordingly. In [15], on the other

		this work	[14]	rel. acc.
$\frac{\Gamma(\eta \rightarrow \pi^+\pi^-e^+e^-)}{\Gamma(\eta \rightarrow \pi^+\pi^-\gamma)}$	(10^{-3})	$6.39^{+0.04}_{-0.06}$	9^{+11}_{-5}	0.9 %
$\frac{\Gamma(\eta' \rightarrow \pi^+\pi^-e^+e^-)}{\Gamma(\eta' \rightarrow \pi^+\pi^-\gamma)}$	(10^{-3})	$7.24^{+0.04}_{-0.10}$	—	1.2 %
$\frac{\Gamma(\eta \rightarrow \pi^+\pi^-\mu^+\mu^-)}{\Gamma(\eta \rightarrow \pi^+\pi^-\gamma)}$	(10^{-7})	$1.61^{+0.38}_{-0.12}$	—	23.1 %
$\frac{\Gamma(\eta' \rightarrow \pi^+\pi^-\mu^+\mu^-)}{\Gamma(\eta' \rightarrow \pi^+\pi^-\gamma)}$	(10^{-5})	$5.4^{+1.6}_{-1.7}$	—	30.9 %

Table 3: Branching ratios of the decay modes into $\pi^+\pi^-l^+l^-$ with respect to the $\pi^+\pi^-\gamma$ decays. The experimental value quoted in the third column is taken from [14]. The relative accuracies of the theoretical results are given in the last column.

hand, a meson exchange model has been employed to calculate numerous decay modes of light unflavored mesons. Despite dissimilarities between [15] and our approach the numerical results are in reasonable agreement. We point out that—in contrast to our work—no theoretical error estimates are given in [15, 24, 25].

The ratios between the $\pi^+\pi^-l^+l^-$ and $\pi^+\pi^-\gamma$ decay channels are given in Tab. 3. The small theoretical uncertainties for the decays into an e^+e^- pair are further reduced down to about 1% in these ratios, while the theoretical accuracies for the $\mu^+\mu^-$ decay ratios remain roughly unaffected. This indicates that the $\pi^+\pi^-e^+e^-$ and $\pi^+\pi^-\gamma$ decays are correlated which can be traced back to the shape of the QED part $\Gamma(\gamma^* \rightarrow e^+e^-)/(k^2\sqrt{k^2})$ in Eq. (6) describing the transition $\gamma^* \rightarrow e^+e^-$. This function possesses a pronounced peak at the virtual photon mass $k_e^2 = (1 + \sqrt{21})m_e^2 \approx 5.6m_e^2$ and projects out the values of the subprocesses $\eta^{(\prime)} \rightarrow \pi^+\pi^-\gamma^*$ at k_e^2 —close to the photon on-shell point $k^2 = 0$. For the $\mu^+\mu^-$ decays, on the other hand, the respective value $k_\mu^2 = (1 + \sqrt{21})m_\mu^2 \approx 5.6m_\mu^2$ is relatively far apart from $k^2 = 0$ so that these decays are not immediately correlated to the $\pi^+\pi^-\gamma$ decays. We observe that for photon virtualities which are not too close to the upper boundary of phase space the rate $\Gamma(\eta^{(\prime)} \rightarrow \pi^+\pi^-\gamma^*)$ in our approach can be very well approximated by a Gaussian of the form $\Gamma(\eta^{(\prime)} \rightarrow \pi^+\pi^-\gamma) \exp(-k^2/\Lambda^2)$ with $\Lambda = (97.8^{+1.8}_{-2.8})$ MeV and $\Lambda = (167.3^{+4.5}_{-5.2})$ MeV for the η and η' decay, respectively. In combination with the sharply peaked QED part the dependence on the small variations in Λ is further reduced in the branching ratios $\Gamma(\eta^{(\prime)} \rightarrow \pi^+\pi^-e^+e^-)/\Gamma(\eta^{(\prime)} \rightarrow \pi^+\pi^-\gamma)$ resulting in the small relative uncertainties of about 1% mentioned above.

In Figs. 6 and 7 we present our predictions for the $\pi^+\pi^-$ and l^+l^- invariant mass spectra, respectively. The lepton-antilepton spectra are strongly peaked right above threshold, so for illustrational purposes we have multiplied these spectra by a factor k^2 which reduces the otherwise extremely pronounced peak. Due to the tiny branching fractions of the decays into $\pi^+\pi^-\mu^+\mu^-$ it will be experimentally very challenging to measure these kinds of spectra. The spectra of the decays involving an electron-positron pair, however, are likely to be probed at the ongoing experiment [2] at COSY-Jülich.

We reconfirm the findings of [12] regarding the importance of the different coupled channels diagrams in Fig. 3. The by far largest contribution to the decay amplitude stems from $\pi^+\pi^-$

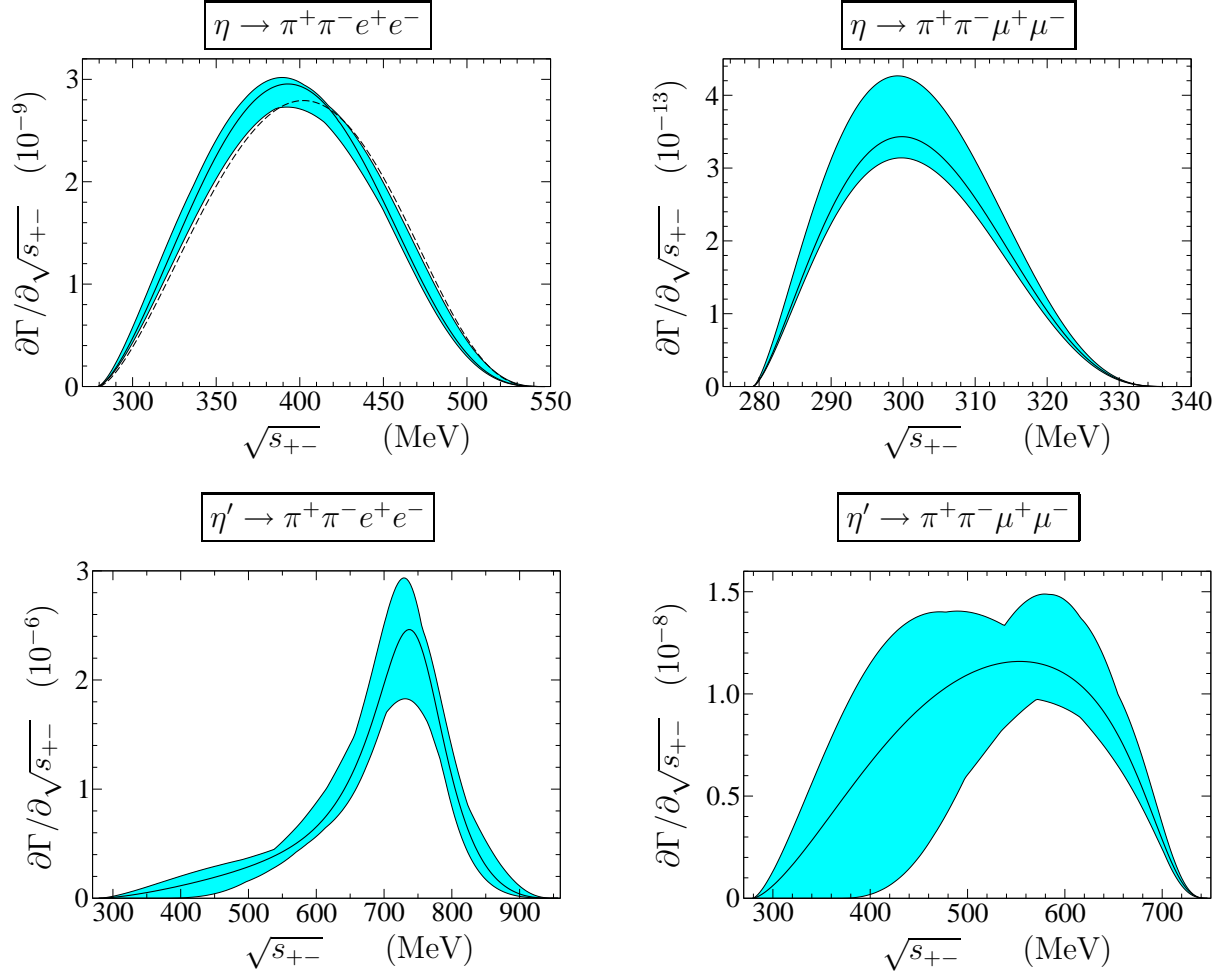


Figure 6: Predicted invariant mass spectra of the $\pi^+\pi^-$ system in the different decay modes. The solid lines represent the fit with minimal χ^2 , the error bands indicate the 1σ confidence region. The result of [25] is represented by the dashed line in the upper left plot.

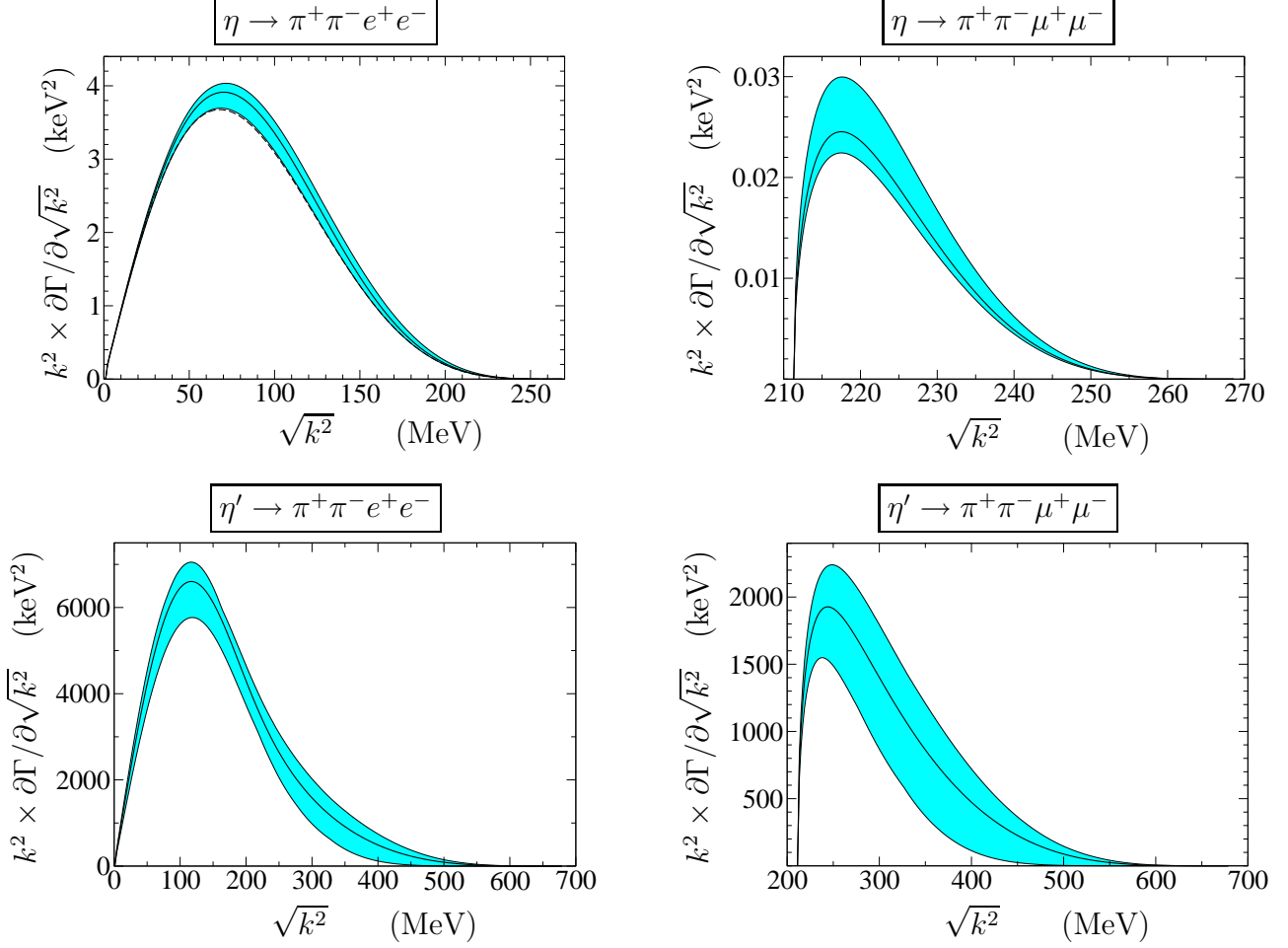


Figure 7: Predicted invariant mass spectra of the lepton-antilepton pair in the different decay modes. The solid lines represent the fit with minimal χ^2 , the error bands indicate the 1σ confidence region. For illustrational reasons the spectra are multiplied by a factor k^2 . The result of [25] is represented by the dashed line in the upper left plot.

	this work	experiment
$\text{BR}(\eta \rightarrow \pi^+\pi^-e^+e^-) \quad (10^{-4})$	$2.99^{+0.08}_{-0.11}$	$4.3 \pm 1.7 \quad [32]$
$\text{BR}(\eta' \rightarrow \pi^+\pi^-e^+e^-) \quad (10^{-3})$	$2.13^{+0.19}_{-0.32}$	—
$\text{BR}(\eta \rightarrow \pi^+\pi^-\mu^+\mu^-) \quad (10^{-9})$	$7.5^{+4.5}_{-2.7}$	—
$\text{BR}(\eta' \rightarrow \pi^+\pi^-\mu^+\mu^-) \quad (10^{-5})$	$1.57^{+0.96}_{-0.75}$	—
$\Gamma(\eta \rightarrow \pi^+\pi^-e^+e^-) \quad (\text{meV})$	389^{+10}_{-13}	$560 \pm 260 \quad [32]$
$\Gamma(\eta' \rightarrow \pi^+\pi^-e^+e^-) \quad (\text{eV})$	431^{+38}_{-64}	—
$\Gamma(\eta \rightarrow \pi^+\pi^-\mu^+\mu^-) \quad (\mu\text{eV})$	$9.8^{+5.8}_{-3.5}$	—
$\Gamma(\eta' \rightarrow \pi^+\pi^-\mu^+\mu^-) \quad (\text{eV})$	$3.2^{+2.0}_{-1.6}$	—

Table 4: This table illustrates how the uncertainties of the results grow if variations of k^2 -dependent counter terms are taken into account.

final-state interactions, *cf.* Fig. 3a, whereas the diagram in Fig. 3d, which mimics the simultaneous exchange of two vector mesons within our approach, yields only small corrections. This is in contrast to the assumption of complete vector meson dominance.

The decay modes $\eta^{(\prime)} \rightarrow \pi^+\pi^-l^+l^-$ involve $\mathcal{O}(p^6)$ counter terms which generate contributions proportional to k^2 and do not contribute to the decays with on-shell photons. Consequently, they cannot be fixed by fitting to $\eta^{(\prime)} \rightarrow \pi^+\pi^-\gamma$ data. In order to examine their impact on the results for $\eta^{(\prime)} \rightarrow \pi^+\pi^-l^+l^-$ we have varied their values in the range $(-10 \dots +10) \times 10^3 \text{ GeV}^{-2}$ which is motivated by the size of the other $\mathcal{O}(p^6)$ couplings, *cf.* Table 2. The enlargement of the error ranges for the branching ratios and widths following from this variation is tabulated in Table 4. It turns out that the influence of the k^2 terms is rather mild for the decays involving an electron-positron pair owing to the fact that the spectra of such decay modes are strongly enhanced at small k^2 , *cf.* Fig. 7. For the decays into $\pi^+\pi^-\mu^+\mu^-$, on the other hand, where k^2 is bounded below by $4m_\mu^2$, the uncertainties from the 1σ confidence regions are roughly doubled by taking into account the counter terms $\bar{w}_{\eta^{(\prime)}}^{(k)}$.

Finally, we show in Tab. 5 the ratios $\Gamma(\eta^{(\prime)} \rightarrow \pi^+\pi^-l^+l^-)/\Gamma(\eta^{(\prime)} \rightarrow \pi^+\pi^-\gamma)$ in the presence of the k^2 terms. The relative uncertainties for the $\mu^+\mu^-$ decays are again approximately doubled with respect to Tab. 3 if these counter terms are taken into account.

6 Conclusions

In this work we have investigated the decays $\eta, \eta' \rightarrow \pi^+\pi^-l^+l^-$ within a chiral unitary approach based on the chiral effective Lagrangian and a coupled-channels Bethe-Salpeter equation. Utilization of the chiral effective Lagrangian guarantees that symmetries and symmetry-breaking patterns of the underlying theory QCD are incorporated in a model-independent fashion. In particular, contributions due to chiral anomalies enter through the Wess-Zumino-Witten Lagrangian. Besides, counter terms of unnatural parity at leading and next-to-leading order are also taken into account.

		this work	[14]	rel. acc.
$\frac{\Gamma(\eta \rightarrow \pi^+\pi^-\ell^+\ell^-)}{\Gamma(\eta \rightarrow \pi^+\pi^-\gamma)}$	(10^{-3})	$6.39^{+0.08}_{-0.11}$	9^{+11}_{-5}	1.6 %
$\frac{\Gamma(\eta' \rightarrow \pi^+\pi^-\ell^+\ell^-)}{\Gamma(\eta' \rightarrow \pi^+\pi^-\gamma)}$	(10^{-3})	$7.24^{+0.09}_{-0.15}$	—	1.9 %
$\frac{\Gamma(\eta \rightarrow \pi^+\pi^-\mu^+\mu^-)}{\Gamma(\eta \rightarrow \pi^+\pi^-\gamma)}$	(10^{-7})	$1.61^{+0.95}_{-0.55}$	—	58.8 %
$\frac{\Gamma(\eta' \rightarrow \pi^+\pi^-\mu^+\mu^-)}{\Gamma(\eta' \rightarrow \pi^+\pi^-\gamma)}$	(10^{-5})	$5.4^{+3.6}_{-2.6}$	—	66.2 %

Table 5: Branching ratios of decay modes into $\pi^+\pi^-\ell^+\ell^-$ with respect to $\pi^+\pi^-\gamma$ decays when k^2 -dependent counter terms are taken into account. The experimental value quoted in the third column is taken from [14]. The relative accuracies of the theoretical results are given in the last column.

We have first performed a full one-loop calculation in ChPT. However, unitarity effects due to final-state interactions are important in η and, in particular, in η' decays and must be treated non-perturbatively. To this aim, meson-meson rescattering is accounted for in a Bethe-Salpeter equation which satisfies exact two-body unitarity.

This method has already been applied successfully to the anomalous decays $\eta^{(\prime)} \rightarrow \gamma^{(*)}\gamma^{(*)}$ and $\eta^{(\prime)} \rightarrow \pi^+\pi^-\gamma$, and to the hadronic decay modes of η and η' . The parameters in our approach are fixed by the latter two processes and meson-meson scattering phase shifts, so that we obtain predictions for the decay widths and spectra of $\eta, \eta' \rightarrow \pi^+\pi^-\ell^+\ell^-$. The decay of η into $\pi^+\pi^-\ell^+\ell^-$ is currently under investigation at KLOE@DAΦNE and a precise check of our prediction for the branching ratio $\Gamma(\eta \rightarrow \pi^+\pi^-\ell^+\ell^-)/\Gamma(\eta \rightarrow \pi^+\pi^-\gamma)$ will soon be available [33]. Similar investigations are also planned at WASA in Jülich [2].

Acknowledgments

We thank Caterina Bloise for useful discussions and Ulf-G. Meißner for reading the manuscript. This research is part of the EU Integrated Infrastructure Initiative Hadron Physics Project under contract number RII3-CT-2004-506078. Work supported in part by DFG (SFB/TR 16, “Subnuclear Structure of Matter”, and BO 1481/6-1).

A $\mathcal{O}(p^6)$ contact term contributions to $\eta^{(\prime)} \rightarrow \pi^+\pi^-\gamma^*$

There are several terms in the unnatural parity part of the effective Lagrangian of sixth chiral order which contribute to $\eta^{(\prime)} \rightarrow \pi^+\pi^-\gamma^*$ at tree level. The full set of Lagrangian terms in the SU(3) framework can be found in [34], whereas in the extended U(3) framework—necessary to describe η' decays—the terms relevant for $\eta^{(\prime)} \rightarrow \pi^+\pi^-\gamma$ have been given in [12]. In this appendix we repeat the construction of the pertinent Lagrangian terms extending the findings of [12] to the description of off-shell photons.

The building blocks for the construction of the chiral Lagrangian read

$$\begin{aligned}\tilde{P}_{\mu\nu} &= U^\dagger \tilde{R}_{\mu\nu} U + \tilde{L}_{\mu\nu} , & \tilde{Q}_{\mu\nu} &= U^\dagger \tilde{R}_{\mu\nu} U - \tilde{L}_{\mu\nu} , \\ M &= U^\dagger \chi + \chi^\dagger U , & N &= U^\dagger \chi - \chi^\dagger U , \\ C_\mu &= U^\dagger D_\mu U , & E_{\mu\nu} &= U^\dagger D_\mu D_\nu U - (D_\mu D_\nu U)^\dagger U ,\end{aligned}\tag{A.1}$$

where $\tilde{R}_{\mu\nu}$, $\tilde{L}_{\mu\nu}$ are the field strength tensors of the right- and left-handed external fields, respectively, the quantity χ involves the quark mass matrix $\mathcal{M} = \text{diag}(\hat{m}, \hat{m}, m_s)$ (with $\hat{m} = (m_u + m_d)/2$), and $D_\mu U$ is the covariant derivative of the meson field U , see [11] for the definitions.

The terms of $\mathcal{O}(p^6)$ relevant for the present work are given by

$$\begin{aligned}\mathcal{L}^{(6)} &= \epsilon^{\mu\nu\alpha\beta} \Big\{ \bar{W}_7 \langle N (\tilde{P}_{\mu\nu} C_\alpha C_\beta + C_\alpha C_\beta \tilde{P}_{\mu\nu} + 2C_\alpha \tilde{P}_{\mu\nu} C_\beta) \rangle \\ &\quad + \bar{W}_8 (\langle M C_\mu \rangle \langle C_\nu \tilde{Q}_{\alpha\beta} \rangle + \langle N \rangle \langle \tilde{P}_{\mu\nu} C_\alpha C_\beta \rangle) \\ &\quad + \bar{W}_9 (\langle M (\tilde{Q}_{\mu\nu} C_\alpha + C_\alpha \tilde{Q}_{\mu\nu}) \rangle + \langle N (\tilde{P}_{\mu\nu} C_\alpha - C_\alpha \tilde{P}_{\mu\nu}) \rangle) \langle C_\beta \rangle \\ &\quad + \bar{W}_{10} \langle M \rangle \langle \tilde{Q}_{\mu\nu} C_\alpha \rangle \langle C_\beta \rangle + \bar{W}_{11} \langle \tilde{P}_{\mu\nu} (E^\lambda_\alpha C_\beta C_\lambda - C_\lambda C_\beta E^\lambda_\alpha) \rangle \\ &\quad + \bar{W}_{12} \langle \tilde{P}_{\mu\nu} (E^\lambda_\alpha C_\lambda C_\beta - C_\beta C_\lambda E^\lambda_\alpha) \rangle + \bar{W}_{13} \langle \tilde{P}_{\mu\nu} (E^\lambda_\alpha C_\lambda - C_\lambda E^\lambda_\alpha) \rangle \langle C_\beta \rangle \\ &\quad + \bar{W}_{14} \langle \tilde{P}_{\mu\nu} (E^\lambda_\alpha C_\beta - C_\beta E^\lambda_\alpha) \rangle \langle C_\lambda \rangle \Big\} .\end{aligned}\tag{A.2}$$

The coefficients \bar{W}_i are even functions of the singlet field η_0 and can be expanded in terms of η_0 ,

$$\bar{W}_i\left(\frac{\eta_0}{f}\right) = \bar{w}_i^{(0)} + \bar{w}_i^{(2)} \frac{\eta_0^2}{f^2} + \bar{w}_i^{(4)} \frac{\eta_0^4}{f^4} + \dots\tag{A.3}$$

with expansion coefficients $\bar{w}_i^{(j)}$ not fixed by chiral symmetry. At tree level we find the following contribution to the amplitude of $\eta^{(\prime)} \rightarrow \pi^+ \pi^- \gamma^*$

$$\mathcal{A}^{(ct)}(\eta^{(\prime)} \rightarrow \pi^+ \pi^- \gamma^*) = -e k_\mu \epsilon_\nu p_\alpha^+ p_\beta^- \epsilon^{\mu\nu\alpha\beta} \frac{1}{4\pi^2 f^3} \beta_{\eta^{(\prime)}}^{(ct)}\tag{A.4}$$

with

$$\begin{aligned}\beta_\eta^{(ct)} &= \frac{64\pi^2}{\sqrt{3}} \Big\{ -4\bar{w}_7^{(0)} m_\pi^2 + 8\bar{w}_8^{(0)} (m_K^2 - m_\pi^2) \\ &\quad + \bar{w}_{11}^{(0)} (m_\eta^2 - 2m_\pi^2 + 2s_{+-} - k^2) - \bar{w}_{12}^{(0)} (2m_\pi^2 - s_{+-}) \Big\} , \\ \beta_{\eta'}^{(ct)} &= 32\pi^2 \sqrt{\frac{2}{3}} \Big\{ 8(-\bar{w}_7^{(0)} + 3\bar{w}_9^{(0)}) m_\pi^2 + (4\bar{w}_8^{(0)} + 6\bar{w}_{10}^{(0)}) (2m_K^2 + m_\pi^2) \\ &\quad + 2\bar{w}_{11}^{(0)} (m_{\eta'}^2 - 2m_\pi^2 + 2s_{+-} - k^2) + 3\bar{w}_{14}^{(0)} (m_{\eta'}^2 + s_{+-} - k^2) \\ &\quad - 2(\bar{w}_{12}^{(0)} + 3\bar{w}_{13}^{(0)}) (2m_\pi^2 - s_{+-}) \Big\} .\end{aligned}\tag{A.5}$$

By defining the combinations

$$\begin{aligned}
\bar{w}_\eta^{(m)} &= -2(2\bar{w}_7^{(0)} + \bar{w}_{11}^{(0)} + \bar{w}_{12}^{(0)})m_\pi^2 + 8\bar{w}_8^{(0)}(m_K^2 - m_\pi^2) + \bar{w}_{11}^{(0)}m_\eta^2, \\
\bar{w}_\eta^{(s)} &= 2\bar{w}_{11}^{(0)} + \bar{w}_{12}^{(0)}, \\
\bar{w}_\eta^{(k)} &= -\bar{w}_{11}^{(0)}, \\
\bar{w}_{\eta'}^{(0)} &= 2\bar{w}_{11}^{(0)} + 3\bar{w}_{14}^{(0)} \\
\bar{w}_{\eta'}^{(m)} &= -4(2\bar{w}_7^{(0)} - 6\bar{w}_9^{(0)} + \bar{w}_{11}^{(0)} + \bar{w}_{12}^{(0)} + 3\bar{w}_{13}^{(0)})m_\pi^2 + (4\bar{w}_8^{(0)} + 6\bar{w}_{10}^{(0)})(2m_K^2 + m_\pi^2), \\
\bar{w}_{\eta'}^{(s)} &= 4\bar{w}_{11}^{(0)} + 2\bar{w}_{12}^{(0)} + 6\bar{w}_{13}^{(0)} + 3\bar{w}_{14}^{(0)}, \\
\bar{w}_{\eta'}^{(k)} &= -2\bar{w}_{11}^{(0)} - 3\bar{w}_{14}^{(0)},
\end{aligned} \tag{A.6}$$

which are obviously linearly independent, we arrive at a simple form for the $\beta_{\eta^{(\prime)}}^{(ct)}$:

$$\begin{aligned}
\beta_\eta^{(ct)} &= \frac{64\pi^2}{\sqrt{3}} \left(\bar{w}_\eta^{(m)} + \bar{w}_\eta^{(s)} s_{+-} + \bar{w}_\eta^{(k)} k^2 \right), \\
\beta_{\eta'}^{(ct)} &= 32\pi^2 \sqrt{\frac{2}{3}} \left(\bar{w}_{\eta'}^{(0)} m_{\eta'}^2 + \bar{w}_{\eta'}^{(m)} + \bar{w}_{\eta'}^{(s)} s_{+-} + \bar{w}_{\eta'}^{(k)} k^2 \right).
\end{aligned} \tag{A.7}$$

Since the mass of the η' is counted as zeroth chiral order, the $\bar{w}_{\eta'}^{(0)}$ piece in $\beta_{\eta'}^{(ct)}$ violates the chiral counting scheme. However, as shown in [12], it can be absorbed into the $\mathcal{O}(p^4)$ coupling $w_3^{(1)}$ and in Sec. 3 we have employed the renormalized value, $\beta_{\eta'}^{(ct)} = 32\pi^2 \sqrt{2/3} (\bar{w}_{\eta'}^{(m)} + \bar{w}_{\eta'}^{(s)} s_{+-} + \bar{w}_{\eta'}^{(k)} k^2)$, without changing the notation.

References

- [1] J. Bijnens, in *Chiral Dynamics: Theory and Experiment*, eds. A. M. Bernstein, D. Drechsel and T. Walcher, Mainz (1997), Springer.
- [2] H. H. Adam *et al.* [WASA-at-COSY Collaboration], arXiv:nucl-ex/0411038.
- [3] H. J. Arends [A2 Collaboration], AIP Conf. Proc. **870** (2006) 481.
- [4] T. Capussela [KLOE Collaboration], Acta Phys. Slov. **56** (2005) 341.
- [5] F. Ambrosino *et al.* [KLOE Collaboration], Phys. Lett. B **648** (2007) 267 [arXiv:hep-ex/0612029].
- [6] V. Nikolaenko *et al.* [VES Collaboration], AIP Conf. Proc. **796** (2005) 154.
- [7] V. Dorofeev *et al.* [VES Collaboration], [arXiv:hep-ph/0607044].
- [8] N. Beisert and B. Borasoy, Nucl. Phys. A **716** (2003) 186 [arXiv:hep-ph/0301058].
- [9] B. Borasoy and R. Nißler, Eur. Phys. J. A **26** (2005) 383 [arXiv:hep-ph/0510384].
- [10] B. Borasoy, U.-G. Meißner and R. Nißler, Phys. Lett. B **643** (2006) 41 [arXiv:hep-ph/0609010].

- [11] B. Borasoy and R. Nißler, Eur. Phys. J. A **19** (2004) 367 [arXiv:hep-ph/0309011].
- [12] B. Borasoy and R. Nißler, Nucl. Phys. A **740** (2004) 362 [arXiv:hep-ph/0405039].
- [13] B. R. Holstein, Phys. Scripta T99 (2002) 55.
- [14] W. M. Yao *et al.* [Particle Data Group], J. Phys. G **33** (2006) 1.
- [15] A. Faessler, C. Fuchs and M. I. Krivoruchenko, Phys. Rev. C **61** (2000) 035206 [arXiv:nucl-th/9904024].
- [16] J. Wess and B. Zumino, Phys. Lett. B **37** (1971) 95.
- [17] E. Witten, Nucl. Phys. B **223** (1983) 422.
- [18] Ö. Kaymakçalan, S. Rajeev and J. Schechter, Phys. Rev. D **30** (1984) 594.
- [19] J. Bijnens, Int. J. Mod. Phys. A **8** (1993) 3045.
- [20] R. Kaiser and H. Leutwyler, Eur. Phys. J. C **17** (2000) 623 [arXiv:hep-ph/0007101].
- [21] N. Beisert and B. Borasoy, Eur. Phys. J. A **11** (2001) 329 [arXiv:hep-ph/0107175].
- [22] A. Abele *et al.* [Crystal Barrel Collaboration], Phys. Lett. B **402** (1997) 195.
- [23] S. I. Bityukov *et al.* [GAMS-200 Collaboration], Z. Phys. C **50** (1991) 451.
- [24] C. Picciotto, Phys. Rev. D **45** (1992) 1569.
- [25] C. Picciotto and S. Richardson, Phys. Rev. D **48** (1993) 3395.
- [26] J. A. Oller and U.-G. Meißner, Phys. Lett. B **500** (2001) 263 [arXiv:hep-ph/0011146].
- [27] N. Beisert and B. Borasoy, Phys. Rev. D **67** (2003) 074007 [arXiv:hep-ph/0302062].
- [28] M. Gormley *et al.*, Phys. Rev. D **2** (1970) 501.
- [29] J. G. Layter *et al.*, Phys. Rev. D **7** (1973) 2565.
- [30] G. Höhler *et al.*, Nucl. Phys. B **114** (1976) 505.
- [31] B. Borasoy, U.-G. Meißner and R. Nißler, Phys. Rev. C **74** (2006) 055201 [arXiv:hep-ph/0606108].
- [32] C. Bargholtz *et al.* [CELSIUS-WASA Collaboration], Phys. Lett. B **644** (2007) 299 [arXiv:hep-ex/0609007].
- [33] Talk by R. Versaci at ETA07, http://www.isv.uu.se/etamesonnet/public/docs/peniscola_summary/emnw_proceedings-versaci.pdf
- [34] D. Issler, Report SLAC-PUB-4943, 1990 (unpublished);
R. Akhoury and A. Alfakih, Ann. Phys. (N.Y.) **210** (1991) 81;
H. W. Fearing and S. Scherer, Phys. Rev. D **53** (1996) 315;
J. Bijnens, L. Girlanda and P. Talavera, Eur. Phys. J. C **23** (2002) 539;
T. Ebertshäuser, H. W. Fearing, S. Scherer, Phys. Rev. D **65** (2002) 054033.